Available online at www.sciencedirect.com

ScienceDirect

International Journal of Heat and Mass Transfer 50 (2007) 4568–4580

International Journal of HEAT and MASS TRANSFER

www.elsevier.com/locate/ijhmt

Assessment of dimensionless CHF correlations for subcooled flow boiling in microgravity and Earth gravity

Hui Zhang [a], Issam Mudawar [a,*], Mohammad M. Hasan [b]

[a] *Boiling and Two-phase Flow Laboratory, School of Mechanical Engineering, Purdue University, West Lafayette, IN 47907, USA*
[b] *NASA Glenn Research Center, 21000 Brookpark Road, Cleveland, OH 44135, USA*

Received 20 November 2006; received in revised form 17 March 2007
Available online 4 June 2007

Abstract

A comprehensive review and analysis of prior subcooled flow boiling CHF correlations was conducted to identify those correlations that provide the most accurate predictions for dielectric working fluids and small rectangular flow passages found in electronics cooling applications in both microgravity and Earth gravity. Since most prior correlations were derived from water databases, only those with dimensionless form were deemed potentially suitable for other working fluids. Only a small fraction of these dimensionless correlations were found to tackle other fluids and more complicated flow and heating configurations with acceptable accuracy. These correlations were ranked relative to mean error, mean absolute error, and root mean square error. Better predictions where achieved when correlations were based on the heated diameter rather than the hydraulic diameter because of the ability of the former to better describe vapor development in subcooled flow. Two previous correlations by Hall and Mudawar provided the best overall CHF predictions for both microgravity and Earth gravity.

1. Introduction

Critical heat flux (CHF) refers to a heat transfer limit that triggers a sudden rise in surface temperature and possible catastrophic failure (burnout) of a device in which evaporation or boiling is occurring. In flow boiling, CHF is an important limit to the design and safe-operation of nuclear reactors and other devices in which it is important to extract the maximum amount of heat without the risk of physical burnout. A large volume of experimental and theoretical studies on the CHF phenomenon have been carried out by many researchers, resulting in numerous empirical correlations and a few mechanistic or semi-empirical models. Design engineers typically utilize CHF correlations to insure that the extreme operating conditions for an application maintain heat fluxes safely below CHF. Unfortunately, most existing CHF correlations have been developed using a small number of data points covering a limited range of flow conditions. Consequently, these correlations cannot be extended to other flow conditions without uncertainty.

Published in 1999, the Purdue University – Boiling and Two Phase Flow Laboratory (PU-BTPFL) CHF database was compiled by Hall and Mudawar [1–5] to (a) amass all known water CHF databases for both vertical upflow and horizontal flow in a uniformly heated channel, (b) assess these databases on a point-by-point basis for any erroneous data, (c) compile all known subcooled CHF correlations for water flow in a uniformly heated tube, (d) evaluate these correlations using the CHF database corrected for the erroneous data, and (e) develop of a simple, subcooled CHF correlation that is superior in accuracy to existing correlations and look-up tables. The PU-BTPFL CHF database has become an effective tool for assessment of the accuracy of newly proposed correlations or models.

The vast majority of published CHF data are for water flows because of applications such as nuclear reactors and conventional steam power plants. However, the past three decades have witnessed rising interest in new applications

* Corresponding author. Tel.: +1 765 494 5705; fax: +1 765 494 0539.
E-mail address: mudawar@ecn.purdue.edu (I. Mudawar).

0017-9310/$ - see front matter © 2007 Elsevier Ltd. All rights reserved.
doi:10.1016/j.ijheatmasstransfer.2007.03.030

Nomenclature

A	flow area of channel
Bo	boiling number, q''_m/Gh_{fg}
C	empirical constant for a specific correlation
C_j	empirical constant or function for a specific correlation, $j = 1, 2, \ldots$
$c_{p,f}$	liquid specific heat at constant pressure
D	inside diameter of tube
D_e	hydraulic equivalent diameter, $4A/P$
D_h	heated equivalent diameter, $4A/P_h$
f	fully developed turbulent flow (Fanning) friction factor for total flow assumed liquid
f_{TP}	two-phase Fanning friction factor
G	mass velocity
g_e	Earth's gravitational acceleration
h	enthalpy of fluid
h_d	liquid enthalpy at point of bubble detachment
h_f	enthalpy of saturated liquid
h_{fg}	latent heat of vaporization
h_g	enthalpy of saturated vapor
h_{SP}	convection heat transfer coefficient for total flow assumed liquid
k_f	thermal conductivity
L	heated length of tube
n	empirical exponent for a specific correlation
Nu_D	Nusselt number for total flow assumed liquid, $h_{\mathrm{SP}}D/k_f$
P	pressure; perimeter
P_{cr}	critical pressure
Pe	Peclet number, $Re_D Pr_f = GDc_{p,f}/k_f$
P_h	heated perimeter
p_r	reduced pressure, P/P_{cr}
Pr_f	liquid Prandtl number, $c_{p,f}\mu_f/k_f$
q''_m	critical heat flux (CHF)
$q'_{m,\mathrm{sat}}$	saturated flow boiling CHF with zero local quality
Re_D	Reynolds number, GD/μ_f
T	temperature
T_{i}	bulk liquid temperature at inlet
T_{sat}	saturation temperature
ΔT_{sub}	liquid subcooling, $T_{\mathrm{sat}} - T$, with saturation temperature evaluated at pressure associated with the CHF data point (usually outlet pressure)
$\Delta T_{\mathrm{sub,o}}$	liquid subcooling at outlet of flow channel
We_D	Weber number, $G^2D/\rho_f\sigma$
x	thermodynamic equilibrium quality, $(h - h_f)/h_{fg}$, with saturated thermo-physical properties evaluated at pressure associated with the CHF data point (usually outlet pressure) unless specifically stated otherwise
x'	true vapor mass fraction in subcooled flow
$x_{\mathrm{i},}{}^*$	pseudo-inlet quality, $(h_{\mathrm{i}} - h_{f,\mathrm{o}})/h_{fg,\mathrm{o}}$, with saturated thermophysical properties evaluated at outlet pressure
Y	dimensionless group for a specific correlation

Greek symbols

α	void fraction
μ	dynamic viscosity
ν	kinematic viscosity
ρ	density
σ	surface tension

Subscripts

CHF	at critical heat flux
f	saturated liquid
g	saturated vapor
h	heated
i	inlet; beginning of heated length
meas	measured value
o	outlet; end of heated length
pred	predicted value
sat	saturated conditions
SP	single-phase flow
sub	subcooled conditions
*	modified parameter for a specific correlation

that preclude the use of water as working fluid. Such is the case with most cooling systems intended for high-performance electronic and power devices. The need to dissipate large heat fluxes while maintaining relatively low device temperatures often requires direct contact of a low-boiling-point coolant with the current-carrying device. Only a few families of coolants can safely achieve this direct contact. These coolants possess excellent dielectric properties and are often inert to most materials found in electronic packages. Unfortunately, key thermophysical properties of these coolants that are responsible for the effectiveness of heat removal (e.g., thermal conductivity and latent heat of vaporization) are far inferior to those of water. Therefore, CHF is a key concern with these coolants; hence the need to accurately determine this limit for these new applications.

Microgravity poses another unique challenge for the design of space-based electronic cooling systems. High cost and complexity have greatly limited the number of published studies on flow boiling in microgravity [6–10]. Of these studies, only a small subset concern flow-boiling CHF. Recently, the authors of the present study presented a series of studies concerning the effects of body force on flow boiling CHF [11–16]. Experiments were first performed at different flow orientations in Earth gravity to explore the relative importance of inertia, surface tension force, and body force on CHF. Microgravity experiments were then performed in parabolic flight trajectory.

Dielectric coolant FC-72 was used as working fluid in all these experiments. The authors also proposed a theoretical method for predicting near-saturated flow boiling CHF that was based on the Interfacial Lift-off Model [15]. In its basic form, this model could not tackle subcooled boiling conditions, given the difficulty of determining the partitioning of wall energy between sensible and latent heat in subcooled flow. They therefore developed a correlation for energy partitioning that enabled extension of the Interfacial Lift-off Model to subcooled conditions [16].

The present study provides an alternate method to determining CHF for subcooled flow boiling of dielectric coolants in both microgravity and Earth gravity. New data were measured in both environments and the effects of microgravity are accounted for with the aid of a new correlation that seeks $1g_e$ equivalent CHF values for the μg_e data. Both the $1g_e$ data and equivalent μg_e data are then compared to the predictions of prior subcooled flow-boiling CHF correlations to assess the accuracy of these correlations in predicting dielectric coolant data for both environments. To ensure applicability for different coolants, only correlations that were developed in dimensionless form are examined. Correlations are then ranked with respect to predictive accuracy.

2. Subcooled FC-72 flow boiling CHF database

CHF values were measured for FC-72 in both microgravity and Earth gravity using the same experimental facility. At the heart of this facility was the flow boiling module illustrated in Fig. 1(a) and (b). This module was formed by bolting together two transparent polycarbonate plastic (Lexan) plates between two aluminum support plates. As shown in Fig. 1(a), a 5.0 × 2.5 mm rectangular slot was milled into the underside of the top plate to form the flow channel. Flush mounted with the upper surface of the bottom plate, the heated wall consisted of a series of resistive heaters that were soldered to the underside of a 0.56 mm thick oxygen-free copper plate as illustrated in Fig. 1(b).

Fig. 2(a) shows a schematic diagram of the two-phase flow loop. This compact loop delivered FC-72 liquid to the test module at the desired flow rate, pressure and temperature. The coolant was circulated through the loop with the aid of a centrifugal pump. The liquid passed through a filter, followed by a turbine flowmeter and an in-line electrical heater before entering the test module. Heat was removed from the fluid by an air-cooled heat exchanger situated downstream from the flow-boiling module. Pressure control was achieved with the aid of an accumulator that was pre-charged with nitrogen gas. Bellows inside the accumulator allowed for thermal expansion and contraction of the working fluid while maintaining a constant pressure reference point for the loop. The charging system shown in Fig. 2(a) was only used during initial deaeration of the fluid. This system was removed following the deaeration

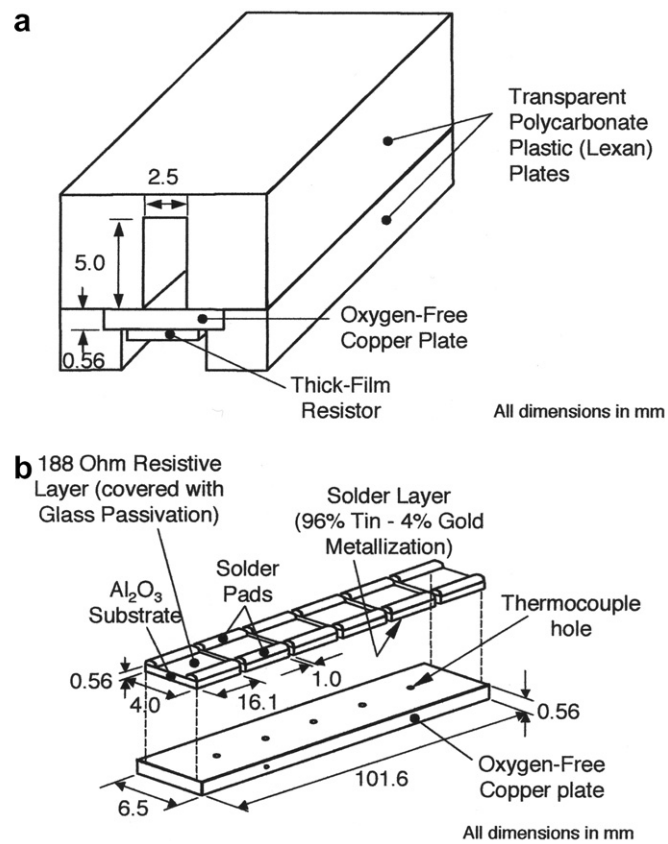

Fig. 1. (a) Flow channel assembly and (b) construction of heated wall.

and before the facility was loaded onboard the aircraft. As depicted in Fig. 2(b), the entire test facility, including the flow loop components, power and instrumentation cabinets, and data acquisition system, was mounted onto a rigid extruded aluminum frame.

The parabolic flight experiments were conducted onboard a NASA KC-135 and a Boeing 727-200 aircraft of Zero-G Corporation. The reduced gravity environment was achieved by a series of parabolic maneuvers as illustrated in Fig. 3(a). Each parabola included a $1.8g_e$ pull-up, a 23 s microgravity period, and a $1.8g_e$ pullout. Fig. 3(b) shows the variation of acceleration during the parabolic flight.

It is important to emphasize that the μg_e CHF data obtained during the parabolic flight experiments were true steady-state data and not transient or heater-specific data. As explained in [15], the heated wall used in the flight rig was chosen to be thick enough to preclude any CHF dependence on wall thickness. However, the wall also was of such low thermal mass that it reached steady state in less than 5 s, well within the μg_e duration of a parabolic maneuver.

The parabolic flight μg_e CHF data were later repeated at $1g_e$. The boiling module's outlet pressure in both environments was maintained at $P_o = 1.44$ bar (20.9 psi). Also available for the present correlation assessment are FC-72 flow boiling CHF data that were measured by

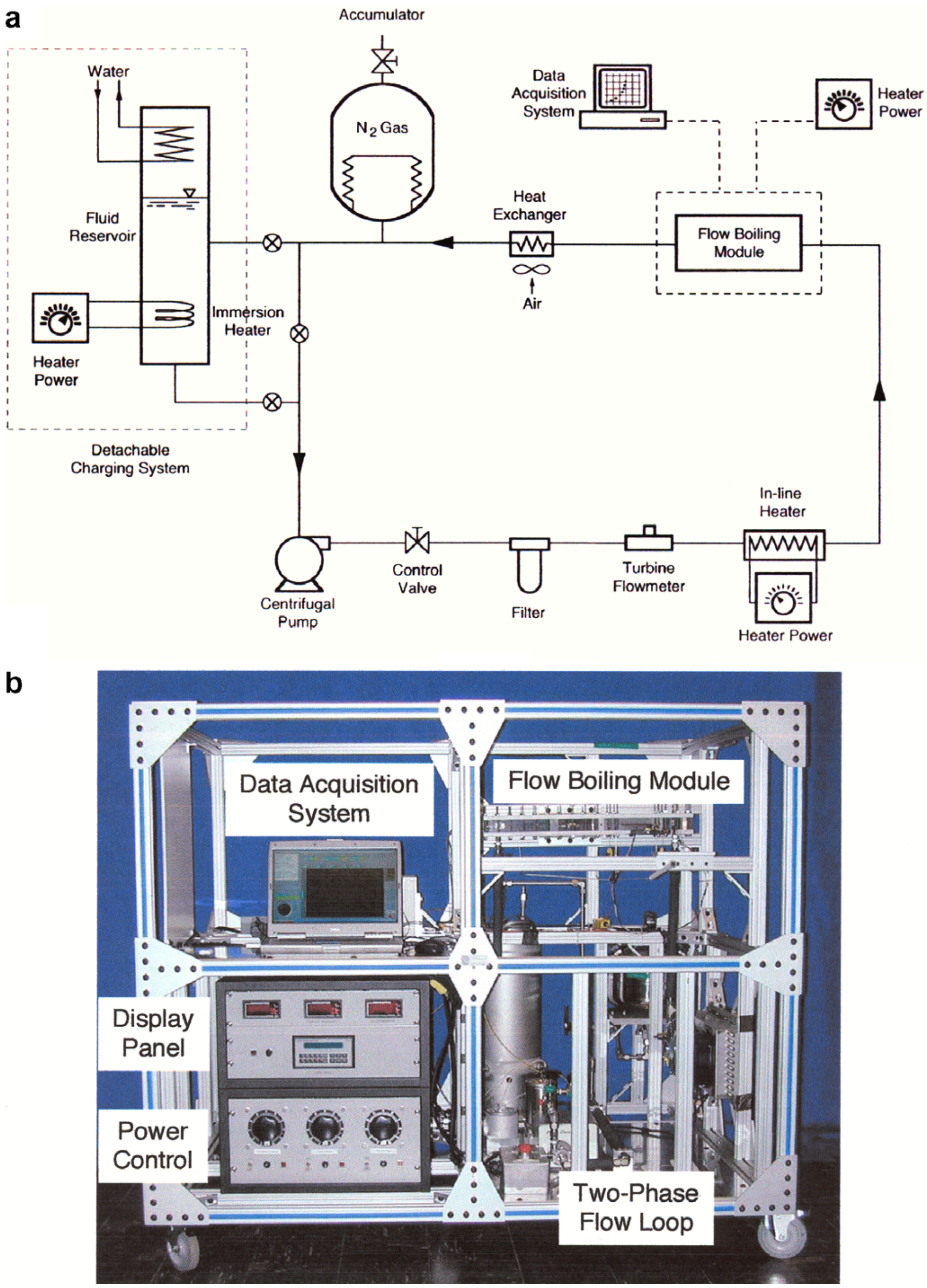

Fig. 2. (a) Schematic of two-phase flow loop and (b) photo of flight apparatus.

Sturgis and Mudawar [17,18] at $1g_e$ using a rectangular flow boiling module having the same dimensions as those of the present study. Outlet pressure for these experiments was maintained at 1.38 bar (20 psi). Tables 1–3 show CHF data from both studies. To preclude any near-saturated outlet conditions, only subcooled CHF data with $\Delta T_{\mathrm{sub,o}} \geqslant 10$ °C were used to evaluate previous subcooled CHF correlations.

Since prior CHF correlations are based entirely on databases measured at $1g_e$, equivalent $1g_e$ CHF values were first obtained for the present μg_e CHF data. Differences between the present μg_e data and the $1g_e$ data obtained in both the present study and by Sturgis and Mudawar were curve-fit, and equivalent $1g_e$ values were obtained for the μg_e data according to the relation

$$\frac{q''_{m,\mathrm{equiv}}}{q''_m} = 1 + 2.15\left(\frac{\rho_f U^2 D_e}{\sigma}\right)^{-0.18}. \tag{1}$$

Table 1 provides both the measured μg_e CHF data and their $1g_e$ equivalent values obtained using Eq. (1).

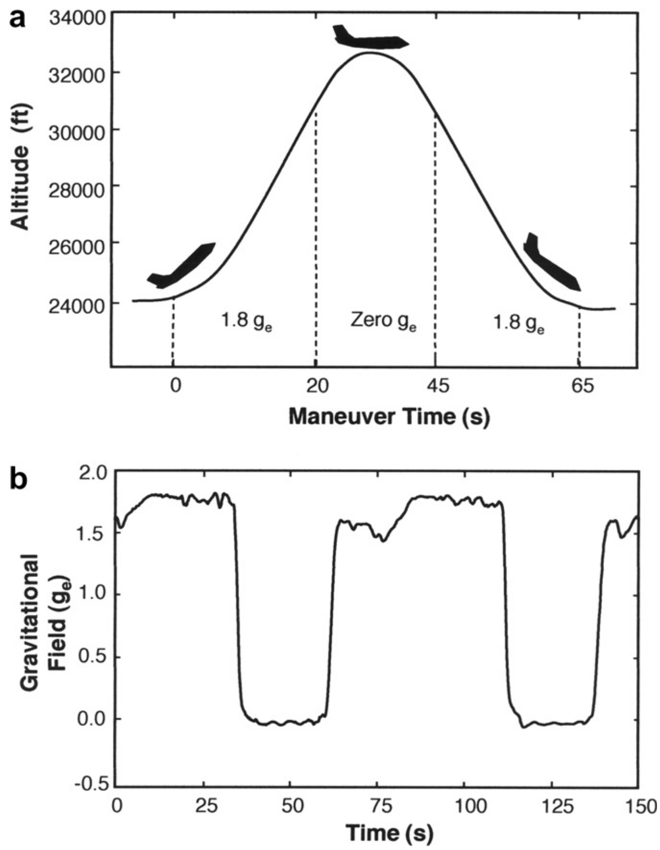

Fig. 3. (a) Trajectory and (b) gravity change of parabolic flight.

Table 1
Present flow boiling CHF data for subcooled FC-72 measured at μg_e, and equivalent $1g_e$ values ($\Delta T_{\mathrm{sub,o}} = 32 \pm 2$ °C)

U (m/s)	Measured q''_m (W/cm^2)	$1 - g_e$ Equivalent q''_m (W/cm^2)
0.30	21.2	42.8
0.50	23.0	42.5
0.60	24.9	44.6
0.70	26.0	45.5
1.10	30.5	49.9
1.50	35.2	55.2

Table 2
Present horizontal flow boiling CHF data for subcooled FC-72 measured at $1g_e$

$\Delta T_{\mathrm{sub,o}} = 10 \pm 2$ °C		$\Delta T_{\mathrm{sub,o}} = 20 \pm 2$ °C		$\Delta T_{\mathrm{sub,o}} = 30 \pm 2$ °C	
U (m/s)	q''_m (W/cm^2)	U (m/s)	q''_m (W/cm^2)	U (m/s)	q''_m (W/cm^2)
0.5	30.1	0.5	31.6	0.5	34.6
0.8	31.3	0.8	33.7	0.8	38.6
1.0	31.9	1.0	35.2	1.0	40.9
1.2	32.5	1.2	37.4	1.2	43.2
1.5	33.1	1.5	40.3	1.5	46.7

3. Compilation of subcooled CHF correlations

CHF correlations are classified as based on either inlet (upstream) conditions or outlet (local) conditions. Inlet conditions correlations are based on pressure, mass flux and inlet enthalpy (or inlet subcooling or quality), in addition to the tube geometry

Table 3
Horizontal flow boiling CHF data for subcooled FC-72 measured by Sturgis and Mudawar [17,18] at $1g_e$

$\Delta T_{\mathrm{sub,o}} = 16$ °C		$\Delta T_{\mathrm{sub,o}} = 29$ °C	
U (m/s)	q''_m (W/cm^2)	U (m/s)	q''_m (W/cm^2)
0.5	35.2	0.5	42.7
0.5	35.5	0.5	43.1
1.0	38.8	1.0	48.8
1.0	38.3	1.0	48.4
1.5	41.8	1.5	54.0
1.5	42.0	1.5	51.5
2.0	44.3	1.5	51.2
2.0	44.0	2.0	59.4
2.0	42.8	3.0	70.7
3.0	47.0	3.0	73.6
4.0	52.4	4.0	86.9
4.0	51.8	5.0	97.1
5.0	63.1	6.0	108.7
6.0	71.7	7.0	118.2
6.0	69.3	8.0	129.3
7.0	76.6		
7.0	76.4		
8.0	85.8		

$$q''_m = f(G, P, h_i, D, L). \tag{2}$$

The parameters in Eq. (2) are independent variables that are readily available for CHF estimation. On the other hand, outlet conditions correlations are based pressure, mass flux, diameter, and an outlet dependent variable such as outlet enthalpy (or outlet subcooling or quality)

$$q''_m = f(G, P, D, h_o). \tag{3}$$

Therefore, use of an outlet conditions correlation involves indirect estimation of CHF since outlet quality must first be calculated using calculating the outlet enthalpy associated with the CHF data point using an energy balance over the entire heated length. This is why tube length does not first appear in Eq. (3).

Using the study by Hall and Mudawar [1–3], the authors of the present study identified all dimensionless CHF correlations applicable to subcooled (i.e., negative outlet quality) flow boiling in a uniformly heated tube. Key equations for the selected correlations are provided in Table 4. Table 5 provides additional important information on each correlation. Multiple rows are utilized where a publication recommended more than one correlation. A correlation is identified as an inlet conditions or outlet conditions correlation. Table 5 also provides the number of adjustable constants in the correlation. These are constants that the author(s) of a correlation varied in pursuit of greater accuracy in CHF prediction. As explained in [1–3], adjustable constants include those appearing in conditional statements that specify the appropriate equation from a set of equations. The condition that a parameter such as outlet quality be either less than or greater than zero is not considered adjustable. The exponent of a parameter in a polynomial function is also not considered adjustable. Table 5 also indicates if a correlation can be used to solve explicitly for CHF or whether it requires iteration. A large number of

Table 4
Subcooled flow boiling CHF correlations

Author(s)	Correlation
Jacobs and Merrill [19]	$\frac{q''_m}{3.1546\times 10^6} = 0.78400 - 0.47962T_* + 0.91581P_* + 1.33762G_* - 4.09246L_* + 2.60341D_* + 0.11501T_*^2 - 0.54502P_*^2 - 0.14804G_*^2 + 0.95825L_*^2 - 0.34693D_*^2 - 0.01258T_*^3 + 0.07398P_*^3 + 0.00643G_*^3 - 0.02242L_*^3 + 0.09933T_*P_* - 0.20015T_*G_* + 0.11052P_*G_* + 0.22063P_*L_* - 0.31924P_*D_* - 0.11436G_*L_* + 0.10575G_*D_* + 0.01732L_*D_* + 0.01384T_*G_*^2,$ $D_* = D/0.00254$ $L_* = L/0.254$ $G_* = G/1356.24$ $P_* = P/(68.9476\times 10^5)$ $T_* = (1.8T_i - 459.67)/100$
Miropol'skii and Shitsman [20]	$\frac{q''_m\mu_f}{\sigma\rho_f h_{fg}} = \begin{cases} \frac{0.174}{3600}\left(\frac{c_{pf}T_{sat}}{h_{fg}}\right)^{0.8}K^{0.4}\left[1-0.45\left(\frac{\rho_f}{\rho_g}\right)^{0.85}x_o\right], & x_o < 0 \\ \frac{0.174}{3600}\left(\frac{c_{pf}T_{sat}}{h_{fg}}\right)^{0.8}K^{0.4}(1-x_o)^n, & x_o \geqslant 0 \end{cases}$ where $K = \left(\frac{G\mu_f}{\sigma\rho_f}\right)\left(\frac{\rho_f}{\rho_g}\right)^{0.2}$ $n = \begin{cases} 0.8, & K \leqslant 0.016 \\ 50K, & 0.016 < K \leqslant 0.06 \\ 3, & K > 0.06 \end{cases}$
Tong [21]	$Bo = (1.76 - 7.433x_o + 12.222x_o^2)Re_D^{-0.6}$
Glushchenko [22]	$Bo = 18.25Pe^{-0.5}\left(\frac{\rho_{f,o}}{\rho_g}\right)^{-0.65}\left(\frac{c_{pf,o}\Delta T_{sub,o}}{h_{fg}}\right)^{0.35}\left(\frac{h_{fg}}{c_{pf,o}T_{sat}}\right)^{1.2}$
Ahmad [23]	$\frac{4Bo(L/D)}{1-x_i} = 1 - \exp\left[-0.522\frac{(1-x_i)^{F/2}}{F}\right]$ where $F = \frac{Y}{(L/D)^{0.6}},$ $Y = \left(\frac{GD}{\mu_f}\right)\left(\frac{\mu_f^2}{\sigma D\rho_f}\right)^{2/3}\left(\frac{\mu_g}{\mu_f}\right)^{0.2} = Re_D\left(\frac{We_D}{Re_D^2}\right)^{2/3}\left(\frac{\mu_g}{\mu_f}\right)^{0.2}$
Levitan and Lantsman [24]	CHF in 8 mm diameter tubes: $q''_{m,*} = 10^6(10.3 - 17.5p_r + 8.0p_r^2)\left(\frac{G}{1000}\right)^{0.68p_r-1.2x_o-0.3}\exp(-1.5x_o)$, CHF for tube diameters other than 8 mm is obtained from $q''_m = q''_{m,*}\left(\frac{0.008}{D}\right)^{0.5}$.
Tong [25]	$Bo = 0.23f_{TP}\left[1 - 0.00216p_r^{1.8}Re_*^{0.5}\left(\frac{\rho_f}{\rho_g}\right)x_o\right]$ where $Re_* = \frac{GD}{\mu_f(1-\alpha)},$ $f_{TP} = 8.0\left(\frac{D}{0.0127}\right)^{0.32}Re_*^{-0.6}$ $\alpha = \frac{Cx'}{1+x'(C-1)},$ $x' = \frac{h_o-h_d}{h_g-h_d},$ $h_d = h_f\left(1 - 6.45\times 10^{-5}\frac{q''_m}{G}\right)$ C is equal to 16 and 10 at 51.7 and 68.9 bars, respectively.
Chernobai [26]	$\frac{8D_*}{Re_D Pr_f}\left(1+1.8\frac{h_f}{h_{fg}}\right)\left(1-\frac{D_*}{Nu_D}\right) = \begin{cases} \frac{\left(Bo + x_o\frac{Nu_D}{Re_D Pr_f}\right)^2}{Bo} & x \leqslant 0 \\ Bo + 2x_o\frac{Nu_D}{Re_D Pr_f}, & x > 0 \end{cases}$ where $D_* = 10\left(\frac{D}{0.004}\right)^{0.5},$ $Nu_D = \frac{(f/2)Re_D Pr_f}{1.07+12.7(f/2)^{0.5}(Pr_f^{2/3}-1)}$ $f = [1.58\ln(Re_D) - 3.28]^{-2}$
Hebel et al. [27]	$q''_m = \frac{GD}{4L}\left\{C_1 h_{fg}\left[1-\exp\left(-2u_{*,1}\frac{\rho_f L}{GD}\right)\right] + C_2 c_{pf}\Delta T_{sub,i}\left[1-\exp\left(-2u_{*,2}\frac{\rho_f L}{GD}\right)\right]\right\},$ where $u^*{}_{,1} = 0.0115(D^*/D)^{0.4}$ $u^*{}_{,2} = 0.08(D^*/D)^{0.4}$ $C_1 = 0.4,\ C_2 = 0.5$

(continued on next page)

Table 4 (*continued*)

Author(s)	Correlation
Ivashkevich [28]	$q''_m = \frac{h_{fg} h_{SP}}{c_{pf}} \left(\frac{1}{0.17+7.4\times10^{-6} Re_D} - 1.5x_o \right)$, where $Nu_D = \frac{h_{SP} D}{k_f} = 0.023 Re_D^{0.8} Pr_f^{0.4}$ $c_{pf}^* = h_f/(T_{sat} - 273.15)$
Inasaka and Nariai [29]	$Bo = \left[1 - \frac{52.3+80x_o-50x_o^2}{60.5+(10^{-5}P)^{1.4}}\right] (1.76 - 7.433x_o + 12.222x_o^2) Re_D^{-0.6}$
Boyd [30]	Boyd presented two correlations: $Bo = 4.728\times10^{-4} + 3.403/Re_D$, $Bo = \frac{30}{Re_D}\left(18.988 \frac{c_{pf}\Delta T_{sub,o}}{h_{fg}} - 1\right)$
Celata et al. [31]	$Bo = (0.216 + 4.74\times10^{-8}P) F Re_D^{-0.5}$ where $F = \begin{cases} 1, & x_o < -0.1 \\ 0.825 + 0.986x_o, & -0.1 < x_o < 0 \\ 1/(2+30x_o), & x_o > 0. \end{cases}$
Hechanova et al. [32]	$Bo = 50\left[1 + 0.0022 p_r^{1.8} Re_D^{0.5} \left(\frac{\rho_f}{\rho_g} \frac{c_{pf}\Delta T_{sub,o}}{h_{fg}}\right)\right] \left(1 + \frac{10}{20+L/D_h}\right) Pr_f^{0.6} Pe^{-0.9}$
Yagov et al. [33]	$q''_m = \frac{q''_{m,sat}}{1+\lvert x_o\rvert} + G c_{pf} \Delta T_{sub,o} \frac{f_*/2}{1-11\sqrt{f_*/2}}$ where $q''_{m,sat} = \begin{cases} \dfrac{0.011 h_{fg}\left(\frac{\sigma^2\rho_g}{v_f D}\right)^{1/3} (Re_D^2 Ff)^{1/10}}{\left[1+4.5\times10^4 \left(\frac{\rho_g v_f^2}{\sigma D}\right)^{3/4} \left(\frac{Re_D^2 f}{F^3}\right)^{1/4}\right]^{1/3}}, & 0.004 \leqslant F < 0.7 \\ 0.001 h_{fg}\left(\frac{\sigma^2\rho_g}{v_f D}\right)^{1/3} (Re_D^2 Ff)^{1/6}, & F \geqslant 0.7 \end{cases}$ $F = \frac{h_{fg}(\rho_g v_f)^{3/2}}{\sigma(k_f T_{sat})^{1/2}}$, $f = [1.58\ln(Re_D) - 3.28]^{-2}$.
Hall and Mudawar [34]	Correlation based on outlet conditions: $Bo = C_1 We_D^{C_2} \left(\frac{\rho_f}{\rho_g}\right)^{C_3} \left[1 - C_4 \left(\frac{\rho_f}{\rho_g}\right)^{C_5} x_o\right]$. Correlation based on inlet conditions: $Bo = \frac{C_1 We_D^{C_2} \left(\frac{\rho_f}{\rho_g}\right)^{C_3} \left[1 - C_4 \left(\frac{\rho_f}{\rho_g}\right)^{C_5} x_{i,*}\right]}{1+4C_1C_4 We_D^{C_2} \left(\frac{\rho_f}{\rho_g}\right)^{C_3+C_5} \left(\frac{L}{D}\right)}$, where $x_{i,*} = \frac{h_i - h_{f,o}}{h_{fg,o}}$, $C_1 = 0.0332$, $C_2 = -0.235$, $C_3 = -0.681$, $C_4 = 0.684$ and $C_5 = 0.832$.
Hall and Mudawar [5]	Correlation based on outlet conditions: $Bo = C_1 We_D^{C_2} \left(\frac{\rho_f}{\rho_g}\right)^{C_3} \left[1 - C_4 \left(\frac{\rho_f}{\rho_g}\right)^{C_5} x_o\right]$ Correlation based on inlet conditions: $Bo = \frac{C_1 We_D^{C_2} \left(\frac{\rho_f}{\rho_g}\right)^{C_3} \left[1 - C_4 \left(\frac{\rho_f}{\rho_g}\right)^{C_5} x_{i,*}\right]}{1+4C_1C_4 We_D^{C_2} \left(\frac{\rho_f}{\rho_g}\right)^{C_3+C_5} \left(\frac{L}{D}\right)}$ where $x_{i,*} = \frac{h_i - h_{f,o}}{h_{fg,o}}$ $C_1 = 0.0722$, $C_2 = -0.312$, $C_3 = -0.644$, $C_4 = 0.900$ and $C_5 = 0.724$

adjustable constants and iteration are an indication of the complexity of a correlation. Table 5 further indicates if the subcooled CHF correlation is also applicable to saturated CHF, fluids other than water, or geometries other than a round tube. Also provided is the additional number of adjustable constants required to predict CHF under these other conditions. Finally, Table 5 provides the earliest and most archival publication of each correlation.

Table 5
Subcooled CHF correlations

Subcooled CHF correlation	Inlet conditions	Outlet conditions	Adjustable constant	Iteration required	Saturated CHF[a]	Multifluid[a]	Multi geometry[a]	Related publications
Jacobs and Merrill [19]	•		24		•			
Miropol'skii and Shitsman [20]		•	6		• 3		• 3	
Tong [21]		•	4		•			Tong et al. [35]
Glushchenko [22]		•	4				•	
Ahmad [23]	•		3		•	•	• 6	
Levitan and Lantsman [24]		•	8		•			Doroshchuk et al. [36,37]
Tong [25]		•	7	•	• 1		•	
Chernobai [26]		•	4	•	•			
Hebel et al. [27]	•		6		•		• 2	Hebel and Detavernier [38]
Ivashkevich [28]	•	3						
Inasaka and Nariai [29]		•	9					Nariai et al. [39], Inasaka and Nariai [40–43], Nariai and Inasaka [44,45], Inasaka [46]
Boyd [30]			•	2				
	–	–	2					
Celata et al. [31]		•	6		• 2			Celata et al. [47–49], Celata [50], Cumo [51]
Hechanova et al. [32]		•	8					
Yagov et al. [33]		•	15				•	Yagov and Puzin [52], Yagov et al. [53], Yagov [54]
Hall and Mudawar [34]		•	5					Bowers [55], Mudawar and Bowers [56]
	•							
Hall and Mudawar [5]		•	5					Bowers [55], Mudawar and Bowers [56], Hall and Mudawar [34]
	•							

Adjustable constants refer to those constants which the authors of a correlation manipulated in order to increase the accuracy of their correlation.
[a] This column identifies those correlations which are valid for a test condition other than water flow in a uniformly heated.

Table 6 provides the parametric range of each correlation. The range of a parameter was either explicitly provided by the author(s) of the correlation or determined by inspection of the published data [1–3].

4. Assessment of CHF correlations

The present study utilized a consistent methodology in assessing the predictive capabilities of the selected subcooled CHF correlations. Because most CHF correlations were developed from databases for water, and since water properties are vastly different from those of FC-72, only dimensionless correlations were assessed with the present FC-72 data. This was a key criterion in identifying the correlations provided in Table 4. Thermophysical properties of FC-72 were evaluated at the temperature specified by the correlation.

Unlike the original data upon which the majority of the selected dimensionless correlations are based, the present FC-72 data involve a partially heated perimeter, i.e., different values of equivalent hydraulic diameter, D_e, and heated diameter, D_h. Therefore, the CHF correlations were assessed twice, first by substituting the tube diameter, D, in a correlation by D_e and then by D_h. One exception was the use of only D_e in Reynolds number to more accurately account for flow characteristics.

Inlet conditions correlations were easier to assess. Here, the inlet parameters required by the correlation are based on the inlet temperature corresponding to the CHF data point. On the other hand, outlet conditions correlations required the calculation of outlet enthalpy, quality or subcooling for each CHF data point using an energy balance. Using the measured value for CHF in this energy balance yielded a true value for the outlet parameter. This method is called the direct substitution method. Another method for determining the value of the outlet parameter is the iterative heat balance method. This later method utilizes numerical iteration to adjust the value of the outlet parameter so that both the predicted CHF and predicted outlet parameter simultaneously satisfy an energy balance and the correlation. The relative merits of the direct substitution method used in the present study is discussed elsewhere [5,57].

Three statistical parameters are used to assess the predictive capabilities of the correlations given in Table 4: mean error, mean absolute error, and root-mean-square (RMS) error, which are defined, respectively, as

Table 6
Recommended parametric ranges for the subcooled CHF correlations

Subcooled CHF correlation (additional parametric range)	$D \times 10^3$ (m)	$L \times 10^3$ (m)	L/D	$G \times 10^{-3}$ ($\mathrm{kg\,m^{-2}\,s^{-1}}$)	$P \times 10^{-5}$ ($\mathrm{N\,m^{-2}}$)	$\Delta T_{\mathrm{sub,i}}$ (°C)	x_{i}	$\Delta T_{\mathrm{sub,o}}$ (°C)	x_{o}
Jacobs and Merrill [19] ($22.2 \leqslant T_{\mathrm{i}} \leqslant 340.0$ °C)	1.91	152.4		0.23	34.5				
	7.77	696.0		10.57	189.6				
Miropol'skii and Shitsman [20][a]	4.00			0.40	34.3				− 0.50
	8.00			10.00	196.1				0.80
Tong [21] ($930 \times 10^3 \leqslant h_{\mathrm{i}} \leqslant 1644 \times 10^3$ J kg^{-1})	5.08	254.0		1.36	68.9				−0.15
	17.78	3657.6		6.78	158.6				0.15
Glushchenko [22]	2.00		10.0	0.50	4.9			25.0	
	12.00		120.0	40.00	197.0			250.0	
Ahmad [23][a]				0.41	1.7				
				9.49	137.9				
Levitan and Lantsman [24]	4.00			0.75	29.4			0.0	0.00
	16.00			5.00	196.1			75.0	0.50
Tong [25][a] ($a \leqslant 0.35$)	5.08			0.68	68.9				−0.25
	45.72			5.97	137.9				0.00
Chernobai [26][a]	0.40			0.40	5.0				−1.75
	37.00			30.00	196.0				0.70
Hebel et al. [27][a] ($T_{\mathrm{i}} \leqslant 320.0$ °C)	0.00	0.0		0.00	20.0				
	30.00	400.0		10.00	200.0				
Ivashkevich [28]	8.00			0.75	29.5			0.0	
	8.00			5.00	98.0			75.0	
Inasaka and Nariai [29][a]	2.00		10.0	0.93	1.0				−0.35
	19.10		190.0	23.10	138.0				−0.00
Boyd [30][a]	3.00			4.60	7.7			30.0	
	3.00			40.60	7.7			75.0	
Celata et al. [31][a]	0.30	2.5		0.90	1.0	90.0			
	25.40	610.0		90.00	84.0	230.0			
Hechanova et al. [32] ($7.0 \times 10^4 \leqslant Pe \leqslant 1.0 \times 10^6$)	5.00		5.0		10.0				
	25.00		80.0		70.0				
Yagov et al. [33][a]	8.00			0.50	15.3				−0.50
	8.00			8.00	200.0				0.00
Hall and Mudawar [34]	0.25			1.52	0.7				−2.13
Outlet conditions correlation	15.00			134.00	196.1				−0.05
	0.25		1.7	1.52	0.7		−2.47		−2.13
Inlet conditions correlation	15.00		96.6	134.00	196.1		−0.04		0.00
Hall and Mudawar [5]	0.25			0.34	1.0				−1.00
Outlet conditions correlation	15.00			30.00	200.0				−0.05
	0.25		1.7	0.34	1.0		−2.00		−1.00
Inlet conditions correlation	15.00		200.0	30.00	200.0		0.00		0.00

[a] Parametric range was incomplete, stated incorrectly, or not explicitly stated by the authors of the correlation in the reference cited. Therefore, the authors of the present study ascertained the parametric range by examining the CHF data (uniformly heated tubes) utilized to develop the correlation or by consulting another publication by the authors of the correlation.

mean error (ME):

$$\frac{1}{N}\sum\frac{q''_{m,\mathrm{pred}} - q''_{m,\mathrm{meas}}}{q''_{m,\mathrm{meas}}} \times 100\%, \tag{4}$$

mean absolute error (MAE):

$$\frac{1}{N}\sum\frac{|q''_{m,\mathrm{pred}} - q''_{m,\mathrm{meas}}|}{q''_{m,\mathrm{meas}}} \times 100\%, \tag{5}$$

and root-mean-square (RMS) error:

$$\sqrt{\frac{1}{N}\sum\left(\frac{q''_{m,\mathrm{pred}} - q''_{m,\mathrm{meas}}}{q''_{m,\mathrm{meas}}}\right)^2} \times 100\%, \tag{6}$$

where N is the number of CHF data points. The mean error provides an indication of the tendency of a correlation to underpredict or overpredict CHF. The mean absolute error treats the absolute error from each data point equally. On the other hand, RMS error assigns greater weight to those predictions exhibiting larger deviation from the experimental value.

Table 7 provides ME, MAE, and RMS error values for each of the correlations given in Table 4. As indicated earlier, the diameter in any Reynolds number in a correlation was replaced by D_e. Correlations containing diameter elsewhere (e.g., in Weber number of length-to-diameter ratio) were tested twice, first using D_e and then using D_h. The diameter that was used to assess the correlation is indicated in Table 7 immediately following the correlation author(s) and reference. Overall, Table 7 shows vast differences in predictive capability among correlations, with some

Table 7
Mean absolute error, mean error, and root-mean-square error of CHF correlations in predicting present CHF data

Correlations	$1g_e$			Equivalent μg_e			$1g_e$ and Equivalent μg_e		
	MAE	ME	RMS	MAE	ME	RMS	MAE	ME	RMS
Jacobs and Merrill [19] (D_e)	3211.0	3211.0	3268.9	2729.4	2729.4	5461.1	3162.0	3162.0	5461.1
Jacobs and Merrill [19] (D_h)	4947.3	4947.3	5036.4	4251.5	4251.5	4252.5	4876.6	4876.6	4962.3
Miropol'skii and Shitsman [20] (D_e)	170.2	170.2	177.1	193.3	193.3	393.1	172.5	172.5	393.1
Tong [21] (D_e)	426.2	426.2	435.0	480.8	480.8	973.9	431.8	431.8	973.9
Glushchenko [22] (D_e)	87.4	−87.4	87.5	89.8	−89.8	179.7	87.7	−87.7	179.7
Ahmad [23] (D_e)	1816.6	1816.6	1825.4	1466.8	1466.8	2974.0	1781.0	1781.0	2974.0
Ahmad [23] (D_h)	5862.5	5862.5	5891.5	4774.8	4774.8	4840.1	5751.8	5751.8	5793.3
Levitan and Lantsman [24] (D_e)	4184.7	4184.7	4408.7	5391.5	5391.5	10797.5	4307.4	4307.4	10797.5
Levitan and Lantsman [24] (D_h)	2373.8	2373.8	2505.3	3070.5	3070.5	3074.8	2444.6	2444.6	2568.9
Chernobai [26] (D_e)	96.9	−96.9	97.0	98.6	−98.6	197.1	97.1	−97.1	197.1
Chernobai [26] (D_h)	97.8	−97.8	97.8	99.0	−99.0	99.0	97.9	−97.9	97.9
Hebel et al. [27] (D_e)	206.5	206.5	219.5	255.0	255.0	514.5	211.5	211.5	514.5
Hebel et al. [27] (D_h)	133.1	133.1	153.2	214.8	214.8	216.2	141.4	141.4	160.7
Ivashkevich [28] (D_e)	17.5	−8.7	21.0	27.4	−27.4	61.4	18.5	−10.6	61.4
Inasaka and Nariai [29] (D_e)	193.9	193.9	224.1	361.2	361.2	735.7	210.9	210.9	735.7
Boyd [30] (D_e)	131.5	128.3	173.8	338.4	338.4	681.8	152.5	149.7	681.8
Celata et al. [31] (D_e)	25.6	−25.0	29.7	50.8	−50.8	103.0	28.1	−27.7	103.0
Hechanova et al. [32] (D_e)	145.7	145.7	158.9	136.2	136.2	273.1	144.8	144.8	273.1
Yagov et al. [33] (D_e)	25.9	19.2	29.4	25.4	25.4	56.7	25.8	19.9	56.7
Yagov et al. [33] (D_h)	25.4	18.1	28.9	24.3	24.3	27.4	25.3	18.8	28.8
Hall and Mudawar [34] (inlet, D_e)	18.8	11.4	21.8	14.7	3.6	40.7	18.4	10.6	40.7
Hall and Mudawar [34] (inlet, D_h)	12.8	−8.5	16.8	14.4	−12.3	18.6	12.9	−8.9	17.0
Hall and Mudawar [34] (outlet, D_e)	19.4	6.1	22.6	16.0	4.4	87.1	19.0	6.0	87.1
Hall and Mudawar [34] (outlet, D_h)	18.7	−18.0	24.6	19.5	−19.4	24.7	18.8	−18.2	24.6
Hall and Mudawar [5] (inlet, D_e)	27.8	26.3	33.8	33.4	33.4	37.6	28.3	27.0	37.6
Hall and Mudawar [5] (inlet, D_h)	15.1	−3.1	17.8	11.8	7.3	12.4	14.8	−2.1	17.3
Hall and Mudawar [5] (outlet, D_e)	26.4	22.1	32.4	40.1	40.1	74.8	27.8	23.9	74.8
Hall and Mudawar [5] (outlet, D_h)	17.7	−13.3	21.5	8.5	−0.6	12.1	16.8	−12.0	20.7

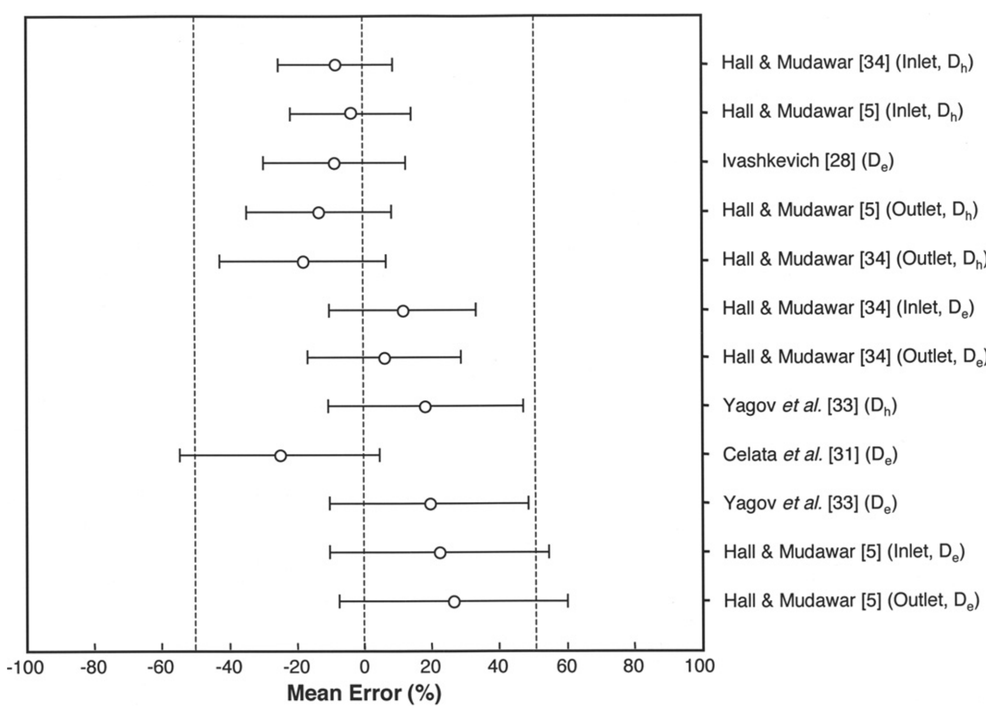

Fig. 4. Mean error and standard deviation for the twelve most accurate subcooled CHF correlations in order of increasing mean absolute error for $1g_e$ CHF data.

providing superior predictions while others yielding unusually large errors. Therefore, only the top twelve best correlations were further examined and compared.

Figs. 4–6 show the mean error and standard deviation from the mean error for the twelve correlations that yielded best predictions of the $1g_e$ data, equivalent μg_e data, and

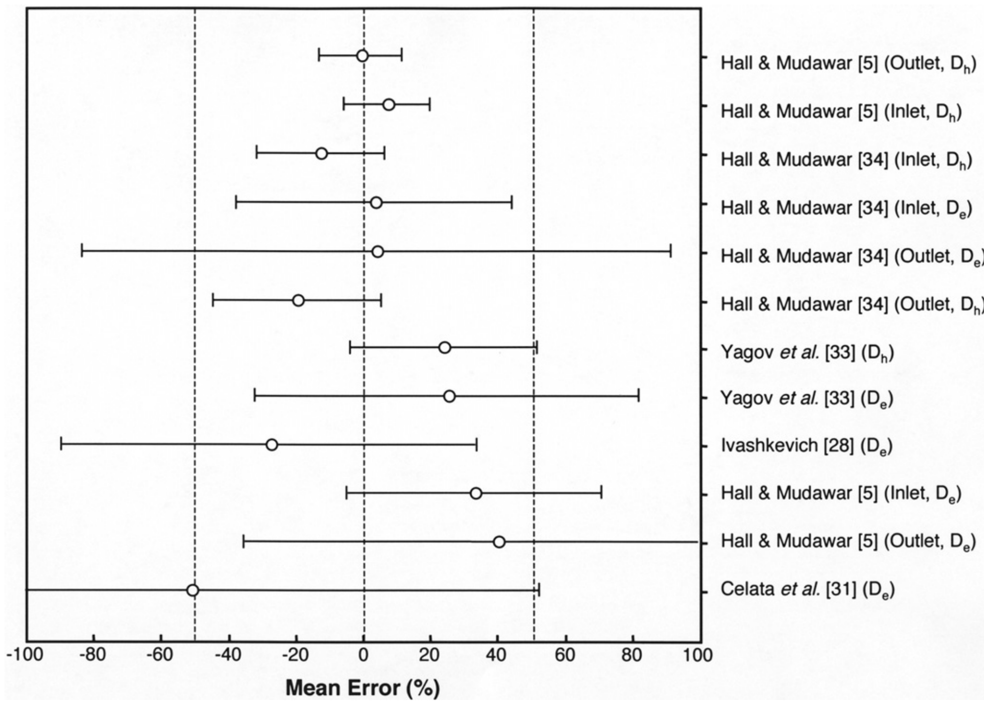

Fig. 5. Mean error and standard deviation for the twelve most accurate subcooled CHF correlations in order of increasing mean absolute error for equivalent μg_e CHF data.

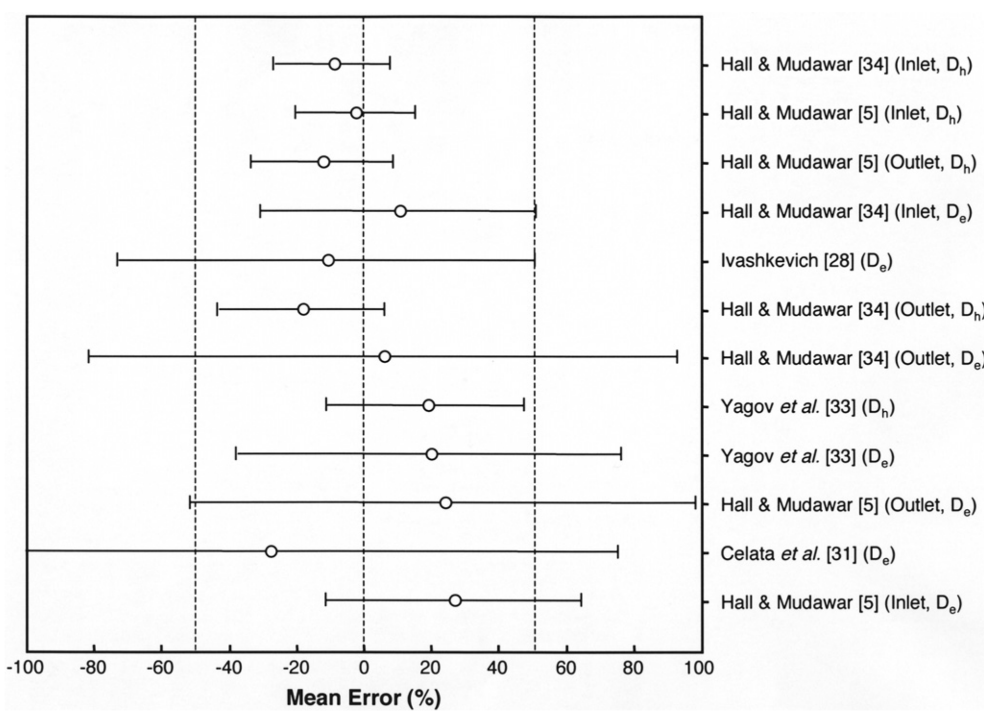

Fig. 6. Mean error and standard deviation for the twelve most accurate subcooled CHF correlations in order of increasing mean absolute error for both $1g_e$ and equivalent μg_e CHF data.

combined $1g_e$ and equivalent μg_e data, respectively, for subcooled FC-72. By definition, CHF predictions for 68% of the data will have errors that lie within a standard deviation from the mean error. Correlations are ranked in each figure in order of increasing mean absolute error. Overall, only five correlations share the best performance for both environments: Hall and Mudawar [5], Hall and Mudawar [34], Ivashkevich [28], Yagov et al. [33], and Celata et al. [31]. Interestingly, those same five correlations were shown by Hall and Mudawar [5] to provide good predictions when tested against all subcooled water data of the PU-BTPFL database. Each of the two correlations by Hall and Mudawar [5,34] can be based on either inlet or outlet conditions, as indicated in Figs. 4–6. Therefore, these two correlations are available in four different forms. Substituting D_e and then D_h in each yields eight possible forms for accuracy assessment. The correlation by Yagov et al. [31] is also tested twice, once using D_e and then D_h. The channel diameter in the correlations by Ivashkievich [28] and Celata et al. [31] appears in Reynolds number terms only; therefore only D_e is used when assessing these two correlations.

Overall, the correlations by Hall and Mudawar [5,34] provide the best predictions, especially when using D_h. This may be the result of the ability of D_h to better account for vapor development along the channel than D_e. Inlet conditions correlations also provide better predictions for the $1g_e$ data, Fig. 4, and combined $1g_e$ and equivalent μg_e data, Fig. 6, but an outlet conditions correlation shows better predictions for the equivalent μg_e data, Fig. 5. Given the relatively small number of μg_e data points, inlet conditions appear better suited for subcooled FC-72. Using the combined databases as basis, Fig. 6, best overall results are achieved using the inlet form of Hall and Mudawar's correlation [34] based on heated diameter, D_h.

5. Conclusions

This study examined prior correlations for subcooled flow boiling CHF, derived mostly from water databases, for suitability to dielectric working fluids and relatively small flow channels found in electronics cooling applications in both microgravity and Earth gravity. Kind findings from this study are as following:

(1) Only dimensionless correlations are deemed suitable for different coolants. Those correlations must also be manipulated by replacing channel diameter by the appropriate hydraulic diameter, D_e, or heated diameter, D_h.
(2) The dimensionless correlations were assessed using several statistical parameters that provide different measures of predictive accuracy. These include mean error, mean absolute error, and RMS error. A subset of the correlations showed good predictive capability while others showed appreciable error. The successful correlations are deemed very effective at correlating CHF data for different fluids and complex flow and heating configurations. Those that yielded poor predictions are not necessarily poor correlations since they were recommended mostly for water flows. Their poor predictive capability is simply an indication that, despite their dimensionless form, they may not be suitable to fluids other than water or to more complicated flow or heating configurations.
(3) Two correlations by Hall and Mudawar [5,34] provide the best overall CHF predictions for $1g_e$ data alone, combined $1g_e$ and equivalent μg_e data, and μg_e data alone, especially when based on inlet conditions. This demonstrates the effectiveness of these correlations at tackling fluids other than water as well as complex flow and heating conditions.

Acknowledgement

The authors are grateful for the support of the National Aeronautics and Space Administration under Grant No. NNC04GA54G.

References

[1] D.D. Hall, I. Mudawar, Critical heat flux (CHF) for water flow in tubes, Compilation and Assessment of the World CHF Data, published by the Boiling and Two-Phase Flow Laboratory, vol. I, Purdue University, West Lafayette, IN, 1999.
[2] D.D. Hall, I. Mudawar, Critical heat flux (CHF) for water flow in tubes, PU-BTPFL CHF Database, published by the Boiling and Two-Phase Flow Laboratory, vol. II, Purdue University, West Lafayette, IN, 1999.
[3] D.D. Hall, I. Mudawar, Critical heat flux (CHF) for water flow in tubes, Subcooled CHF Correlations published by the Boiling and Two-Phase Flow Laboratory, vol. III, Purdue University, West Lafayette, IN, 1999.
[4] D.D. Hall, I. Mudawar, Critical heat flux (CHF) for water flow in tubes – I. Compilation and assessment of world CHF data, Int. J. Heat Mass Transfer 43 (2000) 2573–2604.
[5] D.D. Hall, I. Mudawar, Critical heat flux (CHF) for water flow in tubes – II. Subcooled CHF correlations, Int. J. Heat Mass Transfer 43 (2000) 2605–2640.
[6] M. Saito, N. Yamaoka, K. Miyazaki, M. Kinoshita, Y. Abe, Boiling two-phase flow under microgravity, Nucl. Eng. Des. 146 (1994) 451–461.
[7] Y. Ma, J.N. Chung, An experimental study of forced convection boiling in microgravity, Int. J. Heat Mass Transfer 41 (1998) 2371–2382.
[8] Y. Ma, J.N. Chung, A study of bubble dynamics in reduced gravity forced-convection boiling, Int. J. Heat Mass Transfer 44 (2001) 399–415.
[9] Y. Ma, J.N. Chung, An experimental study of critical heat flux (CHF) in microgravity forced-convection boiling, Int. J. Multiphase Flow 27 (2001) 1753–1767.
[10] H. Ohta, Experiments on microgravity boiling heat transfer by using transparent heaters, Nucl. Eng. Des. 175 (1997) 167–180.
[11] H. Zhang, I. Mudawar, M.M. Hasan, Experimental assessment of the effects of body force, surface tension force, and inertia on flow boiling CHF, Int. J. Heat Mass Transfer 45 (2002) 4079–4095.
[12] H. Zhang, I. Mudawar, M.M. Hasan, Experimental and theoretical study of orientation effects on flow boiling CHF, Int. J. Heat Mass Transfer 45 (2002) 4463–4478.
[13] H. Zhang, I. Mudawar, M.M. Hasan, Investigation of interfacial behavior during the flow boiling CHF transient, Int. J. Heat Mass Transfer 47 (2004) 1275–1288.
[14] H. Zhang, I. Mudawar, M.M. Hasan, A method for assessing the importance of body force on flow boiling CHF, ASME J. Heat Transfer 126 (2004) 161–168.
[15] H. Zhang, I. Mudawar, M.M. Hasan, Flow boiling CHF in microgravity, Int. J. Heat Mass Transfer 48 (2005) 3107–3118.
[16] H. Zhang, I. Mudawar, M.M. Hasan, CHF model for subcooled flow boiling in Earth gravity and microgravity, Int. J. Heat Mass Transfer 50 (19–20) (2007) 4039–4051.

[17] J.C. Sturgis, I. Mudawar, Critical heat flux in a long, rectangular channel subjected to one-sided heating – I. Flow visualization, Int. J. Heat Mass Transfer 42 (1999) 1835–1847.
[18] J.C. Sturgis, I. Mudawar, Critical heat flux in a long, rectangular channel subjected to one-sided heating – II. Analysis of critical heat flux data, Int. J. Heat Mass Transfer 42 (1999) 1849–1862.
[19] R.T. Jacobs, J.A. Merrill, The application of statistical methods of analysis for predicting burnout heat flux, Nucl. Sci. Eng. 8 (1960) 480–496.
[20] Z.L. Miropol'skii, M.E. Shitsman, The critical heat flux for boiling water in tubes, Atomnaya Énergiya 11 (1961) 515–521.
[21] L.S. Tong, Boundary-layer analysis of the flow boiling crisis, Int. J. Heat Mass Transfer 11 (1968) 1208–1211.
[22] L.F. Glushchenko, Correlation of experimental data on critical heat fluxes in subcooled boiling, Teplofizika i Teplotekhnika 15 (1969) 125–129.
[23] S.Y. Ahmad, Fluid to fluid modeling of critical heat flux: a compensated distortion model, Int. J. Heat Mass Transfer 16 (1973) 641–662.
[24] L.L. Levitan, F.P. Lantsman, Investigating burnout with flow of a steam-water mixture in a round tube, Thermal Eng. 22 (1975) 102–105.
[25] L.S. Tong, A phenomenological study of critical heat flux, ASME Paper 75-HT-68, 1975.
[26] V.A. Chernobai, Model for heat-transfer crisis for water boiling in pipes, Teplofizika Vysokikh Temperatur 18 (1980) 1046–1050.
[27] W. Hebel, W. Detavernier, M. Decreton, A contribution to the hydrodynamics of boiling crisis in a forced flow of water, Nucl. Eng. Des. 64 (1981) 433–445.
[28] A.A. Ivashkevich, A semiempirical formula for critical heat flux with boiling of subcooled water in a tube, Thermal Eng. 28 (1981) 303–304.
[29] F. Inasaka, H. Nariai, Critical heat flux and flow characteristics of subcooled flow boiling in narrow tubes, JSME Int. J. 30 (1987) 1595–1600.
[30] R.D. Boyd, Subcooled water flow boiling experiments under uniform high heat flux conditions, Fusion Technol. 13 (1988) 131–142.
[31] G.P. Celata, M. Cumo, A. Mariani, Assessment of correlations and models for the prediction of CHF in water subcooled flow boiling, Int. J. Heat Mass Transfer 37 (1994) 237–255.
[32] A.E. Hechanova, M.S. Kazimi, J.E. Meyer, A framework for critical heat flux prediction in high heat flux, high subcooling components, in: R.J. Cochran, R.E. Hogan, A.M. Khounsary, M.A. Ebadian, M. Kaviany, R.W. Douglass, L.C. Burmeister, J.E. O'Brien, R.L. Mahajan, T.S. Chen, W.J. Bryan, T. Chopin, L.W. Sawnson (Eds.), Proceedings of the ASME Heat Transfer Division, IMECE, San Francisco, California, USA, 1995, pp. 127–132.
[33] V.V. Yagov, V.A. Puzin, L.A. Sukomel, The approximate model for critical heat flux under subcooled flow boiling conditions, in: G.P. Celata, P. Di Marco, A. Mariani (Eds.), 2nd European Thermal-Sciences and 14th UIT National Heat Transfer Conference, Pisa, Italy, 1996, pp. 483–490.
[34] D.D. Hall, I. Mudawar, Ultra-high critical heat flux (CHF) for subcooled water flow boiling – II. High-CHF database and design equations, Int. J. Heat Mass Transfer 42 (1999) 1429–1456.
[35] L.S. Tong, F.E. Motley, J.O. Cermak, Scaling law of flow-boiling crisis, in: U. Grigull, E. Hahne (Eds.), Heat Transfer 1970: Fourth International Heat Transfer Conference, Amsterdam, The Netherlands, 1970, Paper B 6.12.
[36] V.E. Doroshchuk, L.L. Levitan, F.P. Lantsman, Investigations into burnout in uniformly heated tubes, ASME Paper 75-WA/HT-22, 1975.
[37] V.E. Doroshchuk, L.L. Levitan, F.P. Lantsman, Recommendations for calculating burnout in a round tube with uniform heat release, Teploenergetika 22 (12) (1975) 66–70; V.E. Doroshchuk, L.L. Levitan, F.P. Lantsman, Recommendations for calculating burnout in a round tube with uniform heat release, Thermal Eng. 22 (12) (1975) 77–80.
[38] W. Hebel, W. Detavernier, Critical heat transfer rate to flowing cooling water, Kerntechnik 19 (5) (1977) 228–232.
[39] H. Nariai, F. Inasaka, T. Shimura, Critical heat flux of subcooled flow boiling in narrow tube, in: P.J. Marto, I. Tanasawa (Eds.), Proceedings of the 1987 ASME-JSME Thermal Engineering Joint Conference, New York, 1987, pp. 455–462.
[40] F. Inasaka, H. Nariai, Critical heat flux of subcooled flow boiling with water, in: U. Müller, K. Rehme, K. Rust (Eds.), Proceedings of the Fourth International Topical Meeting on Nuclear Reactor Thermal-Hydraulics: NURETH-4, Karlsruhe, Germany, 1989, pp. 115–120.
[41] F. Inasaka, H. Nariai, Critical heat flux of subcooled flow boiling for water in uniformly heated straight tubes, Fus. Eng. Des. 19 (1992) 329–337.
[42] F. Inasaka, H. Nariai, Evaluation of subcooled critical heat flux correlations for tubes with and without internal wwisted tapes, in: Proceedings of the Fifth International Topical Meeting on Reactor Thermal Hydraulics: NURETH-5, La Grange, IL, 1992, pp. 919–928.
[43] F. Inasaka, H. Nariai, Evaluation of subcooled critical heat flux correlations for tubes with and without internal twisted tapes, Nucl. Eng. Des. 163 (1996) 225–239.
[44] H. Nariai, F. Inasaka, Critical heat flux of subcooled flow boiling with water, with application to high heat flux components, Fus. Eng. Des. 9 (1989) 245–249.
[45] H. Nariai, F. Inasaka, Critical Heat Flux and Flow Characteristics of Subcooled Flow Boiling with Water in Narrow Tubes, Dynamics of Two-Phase Flows, CRC Press, Boca Raton, FL, 1992, pp. 689–708.
[46] F. Inasaka, Critical heat flux of subcooled flow boiling in water under uniform heating conditions, Papers Ship Res. Inst. 30 (1993) 1–69.
[47] G.P. Celata, M. Cumo, A. Mariani, CHF in highly subcooled flow boiling with and without turbulence promoters, European Two-Phase Flow Group Meeting, Stockholm, Sweden, June 1–3, 1992, Paper C1.
[48] G.P. Celata, M. Cumo, M.A. Mariani, Burnout in highly subcooled water flow boiling in small diameter tubes, Int. J. Heat Mass Transfer 36 (1993) 1269–1285.
[49] G.P. Celata, M. Cumo, A. Mariani, Experimental results on high heat flux burnout in subcooled flow boiling, Energia Nucl. 10 (1993) 46–57.
[50] G.P. Celata, Recent achievements in the thermal hydraulics of high heat flux components in fusion reactors, Exp. Thermal Fluid Sci. 7 (1993) 263–278.
[51] M. Cumo, Subcooled flow boiling CHF at high liquid velocity, in: Heat Transfer: 3rd UK National Heat Transfer Conference Incorporating 1st European Conference on Thermal Sciences, Hemisphere Pub. Corp., New York, 1992, pp. 15–33.
[52] V.V. Yagov, V.A. Puzin, Burnout under conditions of forced flow of subcooled liquid, Thermal Eng. 32 (1985) 569–572.
[53] V.V. Yagov, V.A. Puzin, A.A. Kudryavtsev, Investigation of the boiling crisis and heat transfer in dispersed-film boiling of liquids in channels, Heat Transfer – Soviet Res. 19 (1987) 1–8.
[54] V.V. Yagov, The mechanism of the heat transfer crisis with saturated and subcooled liquid boiling in tubes, Thermal Eng. 39 (1992) 235–241.
[55] M.B. Bowers, High heat-flux dissipation using small diameter channels, Ph.D. Thesis, Purdue University, West Lafayette, IN, 1994.
[56] I. Mudawar, M.B. Bowers, Parametric study of ultra-high CHF in highly subcooled water flow inside small diameter tubes, in: J.C. Chen, Y. Fujita, F. Mayinger, R. Nelson (Eds.), Convective Flow Boiling, Taylor & Francis, Washington, DC, 1996, pp. 117–122.
[57] X.M. Siman-Tov, Application of energy balance and direct substitution methods for thermal margins and data evaluation, Nucl. Eng. Des. 163 (1996) 249–258.